NAVAL POSTGRADUATE SCHOOL
Monterey, California

THESIS

INTEGRAL HYBRID-BOOST/SOLID-FUEL RAMJET PROPULSION FOR LIGHTWEIGHT TACTICAL MISSILES

by

Paul C. Woods

December, 1995

Thesis Advisor: D. W. Netzer

Approved for public release; distribution is unlimited.

REPORT DOCUMENTATION PAGE

Form Approved OMB No. 0704-0188

1. AGENCY USE ONLY *(Leave blank)*	2. REPORT DATE December 1995	3. REPORT TYPE AND DATES COVERED Engineer's Thesis

4. TITLE AND SUBTITLE INTEGRAL HYBRID-BOOST /SOLID FUEL RAMJET PROPULSION FOR LIGHTWEIGHT TACTICAL MISSILES	5. FUNDING NUMBERS DGAM4 0081
6. AUTHOR(S) Woods, Paul C.	
7. PERFORMING ORGANIZATION NAME(S) AND ADDRESS(ES) Naval Postgraduate School Monterey CA 93943-5000	8. PERFORMING ORGANIZATION REPORT NUMBER
9. SPONSORING/MONITORING AGENCY NAME(S) AND ADDRESS(ES) Ballistic Missile Defense Office, Washington, D.C. 20301	10. SPONSORING/MONITORING AGENCY REPORT NUMBER

11. SUPPLEMENTARY NOTES The views expressed in this thesis are those of the author and do not reflect the official policy or position of the Department of Defense or the U.S. Government.

12a. DISTRIBUTION/AVAILABILITY STATEMENT Approved for public release; distribution is unlimited.	12b. DISTRIBUTION CODE

13. ABSTRACT *(maximum 200 words)*

An investigation was conducted to determine the feasibility of a small, low-cost, caseless, hybrid-booster/solid-fuel ramjet (H/SFRJ) that utilizes a common fuel grain and has no ejectables. Performance of an air-to-ground missile with a solid propellant booster and SFRJ sustainer, capable of being fired from an unmanned aerial vehicle or helicopter was obtained using an Air Force computer code. A H/SFRJ motor was then designed analytically and compared to the generated computer output. The results showed that a H/SFRJ that has performance equal to a solid-booster SFRJ is feasible. The final missile design had a range of 20 nm, a flight Mach number of 2.0, a diameter and length of 5 and 99 inches respectively, and weighed 82 lb. Caseless hybrid rockets with erodible nozzles were tested to validate assumptions made in the design analysis. In addition, transition from hybrid-rocket booster to solid-fuel ramjet sustainer was demonstrated.

14. SUBJECT TERMS Hybrid Rocket, Solid Fuel Ramjet, Tactical Missiles			15. NUMBER OF PAGES 58
			16. PRICE CODE
17. SECURITY CLASSIFICATION OF REPORT Unclassified	18. SECURITY CLASSIFICATION OF THIS PAGE Unclassified	19. SECURITY CLASSIFICATION OF ABSTRACT Unclassified	20. LIMITATION OF ABSTRACT UL

NSN 7540-01-280-5500

Standard Form 298 (Rev.

Prescribed by ANSI Std. 239-18 298-102

INTEGRAL HYBRID-BOOST/SOLID-FUEL RAMJET PROPULSION FOR LIGHTWEIGHT TACTICAL MISSILES

Paul C. Woods
Lieutenant, United States Navy
B.S., University of Washington, 1987

Submitted in partial fulfillment of the
requirements for the degree of

AERONAUTICAL AND ASTRONAUTICAL ENGINEER

from the

NAVAL POSTGRADUATE SCHOOL
DECEMBER 1995

ABSTRACT

An investigation was conducted to determine the feasibility of a small, low-cost, caseless, hybrid-booster/solid-fuel ramjet (H/SFRJ) that utilizes a common fuel grain and has no ejectables. Performance of an air-to-ground missile with a solid propellant booster and SFRJ sustainer, capable of being fired from an unmanned aerial vehicle or helicopter was obtained using an Air Force computer code. A H/SFRJ motor was then designed analytically and compared to the generated computer output. The results showed that a H/SFRJ that has performance equal to a solid-booster SFRJ is feasible. The final missile design had a range of 20 nm, a flight Mach number of 2.0, a diameter and length of 5 and 99 inches respectively, and weighed 82 lb. Caseless hybrid rockets with erodible nozzles were tested to validate assumptions made in the design analysis. In addition, transition from hybrid-rocket booster to solid-fuel ramjet sustainer was demonstrated.

TABLE OF CONTENTS

I. INTRODUCTION

The purpose of this study was to investigate the feasibility of using a caseless missile with a hybrid-rocket booster and a solid-fuel ramjet (SFRJ) sustainer, that have a common fuel and no ejecta, and which can be launched by a unmanned aerial vehicle (UAV) or a helicopter. The design goal was to generate a missile propulsion system that is as inexpensive as possible. Such a missile would support a "Lethal UAV" concept of destroying mobile Theater Ballistic Missile (TBM) launchers. A lethal UAV scenario envisions a UAV loitering autonomously in hostile territory. After receiving cueing, the UAV maneuvers to launch a lightweight (80 lb.) missile which carries a small anti-tank type warhead. The missile accelerates towards its target while receiving updated targeting information from the cueing sensors via a data link.

Any weapon carried aboard a UAV must be extremely lightweight to avoid excessive reduction in UAV endurance. For example, a Predator UAV carrying two Hellfire missiles, weighing approximately 100 lb. each, has a total endurance loss of about 20 hours [Ref. 1, pg. 69].

A missile propulsion system combining an integral hybrid-rocket booster and a SFRJ sustainer offers several potential advantages over the conventional solid rocket motors used in the majority of US tactical missiles today. As shown by Fruge and Netzer, [Ref. 2], SFRJ propulsion can increase the range of a tactical air-to-surface missile by an order of magnitude over what is possible with conventional solid rocket motors without increasing size and weight. Using an integral hybrid-rocket booster vice a conventional solid rocket booster is attractive for a number of reasons. Hybrid propellants are considerably cheaper than solid propellants. Separation of the solid fuel and liquid oxidizer, and the necessity to have oxidizer flow over the fuel surface for combustion in the hybrid rocket, prevents potential explosion hazards during manufacture and operation. Production costs are reduced when typical propellants are used. Also, hybrid fuel grains, made of materials such as polymethylmethacrylate (PMM, commercially available as Plexiglas), are much more rugged than solid propellant

grains. They cannot be over pressurized due to cracks in the propellant and due to debonding of the propellant from the motor case. They are much safer as a result. Other problems that are avoided are the difficulty of bonding the solid propellant to the solid fuel and cold temperature effects on the structural integrity of solid propellants.

An important question to be answered in this study was whether a single fuel that acts as a hybrid booster, and then as a sustainer, is possible. Such a unified fuel grain would reap substantial cost savings by eliminating the casting of the solid-booster propellant inside the sustainer. The unified fuel grain might be strong enough to withstand internal combustion pressure and flight-induced g-loads without the need for a metal case. Removing the metal case and its associated manufacturing would further reduce costs. The internal liner and insulation necessary to protect the metal case would also be eliminated. Fig. 1.1 depicts a typical conventional boost-sustain type missile construction.

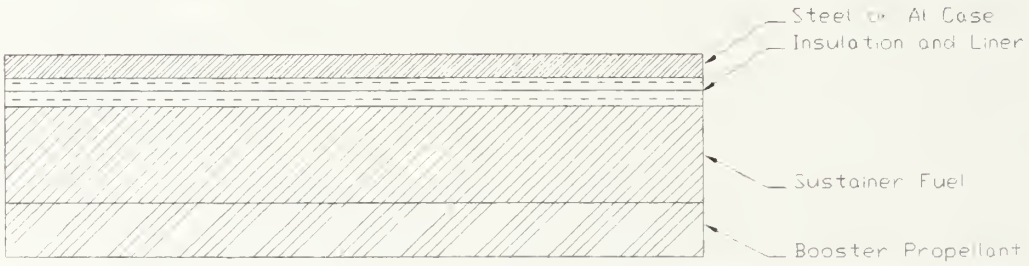

Figure 1.1 Conventional Integral-Rocket SFRJ Missile Construction

Another point of investigation was whether the ejectable booster nozzle could be done away with in favor of a nozzle that erodes during booster operation. Ideally, the nozzle throat would open up to the design area for sustainer operation. Again, the object is to increase simplicity, decrease cost and increase safety (to the launch platform). Nozzleless boosters can be used for solid propellants, but the thrust decays rapidly due to the increasing "throat" size. Except for plateau-burning propellants (n=0) the increased "throat" size results in significantly lower chamber pressures (P_c) since

$$P_c \sim \left(\frac{1}{A_{throat}} \right)^{\frac{1}{1-n}} \tag{1.1}$$

where 'n' is the propellant burning-rate exponent in the expression,

$$\dot{r} = a \cdot P_c^n \tag{1.2}$$

and where $\dot{r}$ is the surface regression rate and 'a' is a constant.

In contrast, hybrid operation is affected less by chamber pressure because the fuel regression rate is practically independent of pressure. So, while some booster performance degradation may be anticipated when using a varying-area nozzle with a hybrid booster, the extent of the degradation must be investigated. The manner in which the nozzle area varies with motor operating conditions is important for optimization of booster performance.

Several concerns must be addressed before using a hybrid rocket as a booster. As pointed out by Marxman [Ref. 3], and others, hybrid rockets suffer from low fuel regression rates, which complicates grain design. The normal method to overcome low regression rate is to use multiple ports; but in small tactical motors of 5 in. to 6 in. diameter, multiple ports may not work well.

Hybrid operation is extremely dependent on the variation of the gas port area and grain geometry. The fuel-to-oxidizer ratio, F/O, typically decreases during operation, and the grain geometry must be optimized so as to increase the burn area sufficiently to operate near the design point over the course of the boost phase. Successfully choosing a grain that works well for the booster does not mean that the sustainer requirements will be met when the boost phase is finished. Careful optimization must be made of grain length, grain cross-sectional shape and port area, oxidizer mass flow, and other parameters, in order to meet mission requirements.

stabilization is
esign from the
RR and the H/SFRJ
nto the code as
of the IRR. The new
ponent weights and

ssile had to be chosen.
load of 25 lb. was set.
l weight carrying
(2).
dizer required for the
ases had to be
ram serves as a
l missiles using solid
newhat
em.
t 2 code. For the
d to define the

. DESIGN METHODOLOGY

to obtain a hybrid/solid-fuel ramjet (H/SFRJ) design starts by
onfiguration: what type of inlet is to be used, constraints on
roperties, etc. After the basic configuration has been
ghts, burn times, and delivered specific impulse required by
on objectives must be obtained. The *Ramjet Engine and*
mjet 2, design code, [Ref. 4], was used for this purpose.
red to analyze integral-rocket ramjets (IRR) and not set up to
rid performance equivalent to that of the IRR must be
able to use the cost and safety advantages of the H/SFRJ, the
d H/SFRJ must be similar. Therefore the weights of the
omponents must be calculated. These include;

investigation was Plexiglas (PMM). PMM is inert,
l machine, and is very inexpensive. It has excellent
uit it for use as a caseless fuel. Yield strength is 7,000-
mperature of PMM is approximately 600 K, which allows it
ber applications (~2.0) without fear of melting. Two
d fuming nitric acid (IRFNA) and gaseous oxygen were

tainer fuel weights are calculated, the grain of the H/SFRJ
proper fuel flow rate. The chosen grain shape is then
heck the actual performance of thrust and total impulse.
d and varying area nozzle. Finally, the chamber Mach

number is checked at sustainer start-up to ensure that proper flame stabilization is possible. The final analytical design is then compared to the IRR design from the computer code. Large differences in required length between the IRR and the H/SFRJ designs are handled by taking the increased length and inputting it into the code as nonpropulsive length and recomputing the theoretical performance of the IRR. The new performance values are used to determine the updated H/SFRJ component weights and grain design. Iteration using this method is very quick.

B. DEFINING REQUIRED MISSILE PERFORMANCE

Prior to beginning this study the basic parameters of the missile had to be chosen. A goal of 20 nm powered range and a speed of Mach 2.0 with a payload of 25 lb. was set. Required missile weight was limited to 80 lb. because of the limited weight carrying capacity of a UAV. A diameter of 5.0 in was selected based on Ref. (2).

To calculate the amount of PMM fuel and the amount of oxidizer required for the booster design, the thrust and total impulse for boost and sustain phases had to be determined. These values were obtained using Ramjet 2. The program serves as a conceptual design tool for air-to-air or air-to-ground ramjet powered missiles using solid rocket motor boosters. Thus, the program had to be utilized in a somewhat unconventional manner to simulate the hybrid/SFRJ propulsion system.

First an IRR baseline missile was generated using the Ramjet 2 code. For the purposes of this study, the following inputs to the program were used to define the missile :

Payload Weight - 22.5 lb
Payload Length - 15 in
Missile Type - Air-to-Surface Missile (ASM)
Wing Planform Area - 0.50 ft^2
Tail Planform Area - 0.25 ft^2
Inlet Type- Chin-Mounted, 2-Dimensional
Case Material - Titanium
Nose Shape - Tangent Ogive
Booster Configuration - IRR
Booster Propellant - Low Smoke
Solid Ramjet Fuel - UTX 18188 (Hydrocarbon)

The payload weight of 22.5 lb included the warhead and guidance. This weight was chosen based on work done in [Ref. 2]. Titanium was chosen as the case material input because it was the closest approximation to the anticipated weight of the excess PMM that would essentially act as the case of the H/SFRJ design.

The information desired from the program was the total impulse produced by both the booster and sustainer, the booster and sustainer burn times, fuel and propellant weights, and SFRJ grain and mixer length. Booster total impulse was not directly calculated but was found from:

$$\text{Total Impulse} = \text{Thrust} \cdot \text{time} \tag{2.1}$$

The designs obtained from Ramjet 2 are given in Table 2.1.

Design Altitude	Boost Thrust (lbf)	Boost Time (sec)	Boost Fuel (lb)	Sustain Isp (sec)	Sustain Time (sec)	Sustain Fuel (lb)
0 ft	1981.2	3.07	23.9	848.6	51.8	22.9
10k ft	1826.5	3.01	21.0	897.2	53.7	15.7
20k ft	1717.4	2.94	18.7	948.2	55.8	10.4
30k ft	1641.1	2.85	16.9	1003.6	58.1	6.8
40k ft	1590.6	2.79	15.7	1032.0	59.8	4.3

Table 2.1 Ramjet 2 Output for 5" Diameter IRR

C. PMM FUEL MASS

Booster

The amount of equivalent PMM fuel (burned with gaseous oxygen or IRFNA) to accomplish the boost phase of the mission using a hybrid rocket was found from the values of required booster total impulse, I_t, calculated by the program. The total amount of booster PMM and oxidizer was given by,

$$m_{total} = \frac{I_t}{Isp \cdot g_o} \tag{2.2}$$

Isp for PMM and the appropriate oxidizer was determined using the aerothermochemical equilibrium program, PEPCode94 [Ref. 4], for a specified fuel-oxidizer ratio (f) and chamber pressure. The amount of oxidizer required by the hybrid booster was,

$$m_{oxidizer} = \frac{m_{total}}{1+f} \tag{2.3}$$

Booster PMM fuel mass was calculated from,

$$m_{fuel} = m_{oxidizer} \cdot f \tag{2.4}$$

An Isp efficiency of 88% was used to account for inefficiencies in the nozzle and in combustion.

Sustainer

The total thrust of the H/SFRJ must match that given by the design code. Net sustain thrust required was determined from Ramjet 2 values for Isp, burn time ($t_{sustainer}$), and fuel mass (assuming constant fuel flow).

$$\text{thrust} = Isp_{fuel} \cdot g_o \cdot \frac{m_{fuel}}{t_{sustainer}} \tag{2.5}$$

PEPCode94 provided jet specific impulse for the combustion of PPM and air, which is related to the exit velocity (u_e) by,

$$Isp_{jet} = \frac{u_e}{g_o} \tag{2.6}$$

Using the momentum equation, the relationship between the thrust output from the design code and the Isp_{jet} was given by

$$\text{thrust} = \left(\dot{m}_{air} + \dot{m}_{fuel}\right) \cdot u_e - \dot{m}_{air} \cdot u_o + A_e \cdot (p_e - p_o) \tag{2.7}$$

where the pressure difference at the nozzle exit (A_e) was set to zero. Substituting for u_e and introducing the fuel-air ratio (f),

$$\text{thrust} = \left(Isp_{jet} \cdot g_o \cdot (1+f) - u_o\right) \cdot \dot{m}_{air} \tag{2.8}$$

The velocity, u_o, was found from the Mach number and speed of sound,

$$u_o = M_o \cdot \sqrt{\gamma \cdot R_o \cdot T_o} \tag{2.9}$$

The fuel-air ratio and chamber pressure, must be specified prior to running the aerothermochemical equilibrium code that determines Isp_{jet}. Equation (2.8) was solved for $\dot{m}_{air}$. The required rate of PMM fuel flow for the sustainer operation followed directly from

$$\dot{m}_{PMM} = f \cdot \dot{m}_{air} \tag{2.10}$$

D. TANKAGE

Having found the booster fuel and oxidizer weights and the sustainer fuel weight, attention is turned to finding the mass of the tanks to contain the boost oxidizer. For gaseous oxygen a blowdown system was used. The analysis for using IRFNA as an oxidizer assumed a regulated pressure system.

IRFNA

Fig. 2.1 depicts a typical pressure-regulated feed system.

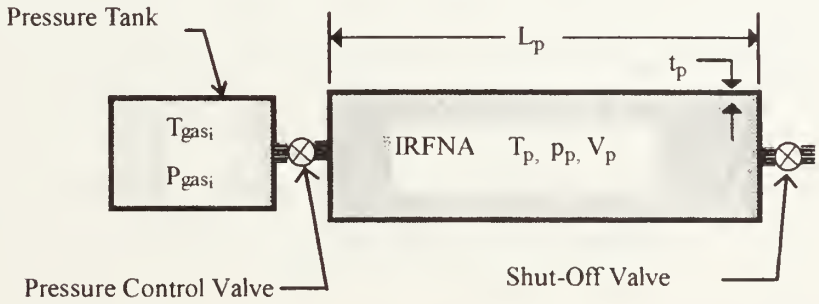

Figure 2.1 Pressure-Regulated Feed

Tank weight for a liquid IRFNA oxidizer was estimated using equations for thin-walled pressure vessels with flat ends. First, tank wall thickness (t_p) and length (Lp) are found using

$$t_p = \frac{p_p \cdot r_p \cdot SF}{\sigma_{yield}} \tag{2.11}$$

and

$$L_p = \frac{\left(\frac{m_{IRFNA}}{\rho_{IRFNA}}\right)}{\pi \cdot r_p^2} \tag{2.12}$$

where r_p is the radius of the tank and SF is a safety factor (taken to be 1.2). The oxidizer tank pressure, p_p, is taken to be the chamber pressure plus 200 psi and the final pressure in the pressurizing tank, p_{gas_f}, is taken to be equal to the oxidizer tank pressure.

The mass of an aluminum tank containing the oxidizer is then determined using

$$m_{tank} = \rho_{Al} \cdot \left[2 \cdot \pi \cdot t_p \cdot L_p \cdot r_p + 2 \cdot t_p \cdot \pi \cdot r_p^2\right] \tag{2.13}$$

In addition to the IRFNA tank weight, the weight of the gas supply tank and pressurizing gas must be determined. Computation of the amount of gas necessary to pressurize the oxidizer tank was made using conservation of energy for the gas as it expands and does work in expelling the liquid oxidizer, [Ref. 6, pg. 324]. The process was assumed to be adiabatic from the initial (subscript 'i') to the final state (subscript 'f'). Therefore

$$m_{gas_f} \cdot c_v \cdot T_{gas_f} + m_p \cdot c_v \cdot T_p + p_p \cdot V_p = m_i \cdot c_v \cdot T_{gas_i} \tag{2.14}$$

$$\frac{c_v \cdot p_{gas_f} \cdot V_i}{R} + \frac{c_v \cdot p_p \cdot V_p}{R} + p_p \cdot V_p = m_i \cdot c_v \cdot T_{gas_i} \tag{2.15}$$

$$\frac{\left(p_{gas_f} \cdot V_i + p_p \cdot V_p \cdot \gamma\right)}{R \cdot T_{gas_i}} = m_i \tag{2.16}$$

Using the perfect gas law, the initial volume of pressurant (V_i) is given by

$$V_i = \frac{m_i \cdot R \cdot T_{gas_i}}{p_i} \tag{2.17}$$

and using Eqn. (2.16), the mass (m_i) of pressurizing gas required is given by

$$m_i = \frac{p_p \cdot V_p}{R \cdot T_{gas_i}} \cdot \left(\frac{\gamma}{1 - \frac{p_{gas_f}}{p_i}} \right) \tag{2.18}$$

The volume of the pressurant was then obtained using Eqn. (2.17). The length and mass of the pressurizing tank could then be found using

$$L_p = \frac{V_i}{\pi \cdot r_p^2} \tag{2.19}$$

and

$$m_{tank} = \rho_{Al} \cdot t_p \cdot 2 \cdot \pi \cdot \left(L_p \cdot r_p + r_p^2 \right) \tag{2.20}$$

where the thickness of the tank wall (t) is found using Eqn. (2.11). Helium was used as the pressurant and the following values were assumed for the above calculations,

R = 8314 joule/kg-K
T = 298 K

Aluminum was used as the tank material. The following values were used for density and yield strength,

ρ_{Al} = 0.161 lb/in^3
σ_{yield} = 1.20e6 psi

Oxygen

To compare with the IRFNA tankage requirements, the weight of a blow-down oxygen feed system was estimated. A blow-down tank has the advantage of being less complex than a comparable pressure-regulated design, because it eliminates one tank and valve, Fig. 2.2. Initial and final pressures in the tank were chosen as 5000 and 2200 psi respectively. The final pressure of 2200 psi was chosen to provide for a constant mass flow through a sonic choke. A pressure ratio of two across the sonic choke was sufficient to ensure a constant mass flow into the hybrid combustor where the pressure was to be approximately 1100 psi.

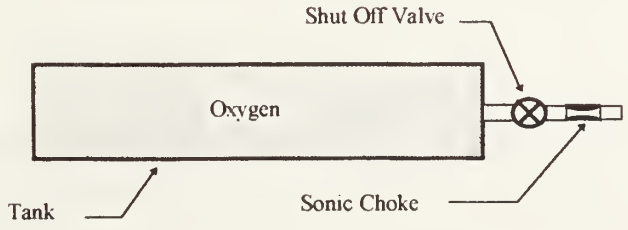

Figure 2.2 Blowdown Feed System

Similar to the pressure-regulated system, the tank wall thickness was given by

$$t = \frac{p \cdot r \cdot SF}{\sigma_{yield}} \tag{2.21}$$

and the volume of the tank was found using the ideal gas equation of state,

$$V = \frac{m_{oxygen} \cdot T \cdot R}{p} \tag{2.22}$$

The total mass of oxygen in the equation above was calculated assuming that the gas temperature was constant such that,

$$V_f = V_i$$

or,

$$m_i \cdot p_f = m_f \cdot p_i \tag{2.23}$$

where the initial mass in the tank was simply the final mass and the mass of oxygen actually used during hybrid operation,

$$m_i = m_f + m_{oxygen} \tag{2.24}$$

which simplifies to,

$$m_i = m_{oxygen} \cdot \left(1 + \frac{p_f}{p_i - p_f}\right) \tag{2.25}$$

Since m_{oxygen} has been calculated in the previous section, the above expression was easily evaluated. The length and mass of the tank were found using Eqn. (2.19) and Eqn. (2.20).

E. FUEL REGRESSION RATE

Hybrid

For this investigation the internal ballistics model developed by Marxman, and others at UTC, [Ref. 3], was used. In this model, solid-fuel regression is controlled by convective heat transfer to the grain. Radiative heat transfer is neglected, but should be minimal since there are no metal particles in the fuel. In this model, combustion takes place in a thin diffusion flame within the boundary layer (Fig 2.3).

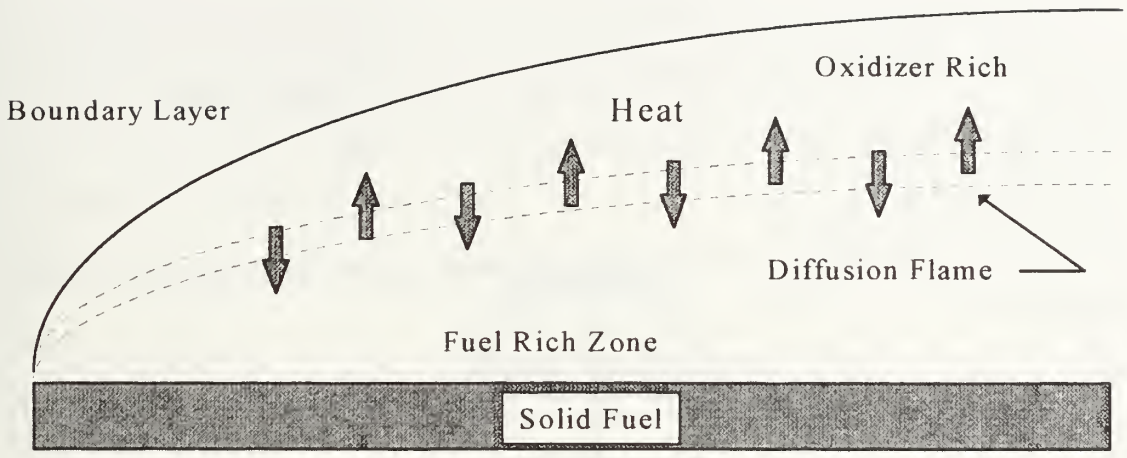

Figure 2.3 Hybrid Combustion Model

In the regression rate model, there is a strong coupling between the heat transferred by convection to the fuel surface and the rate at which fuel is injected into the flow. Increasing the energy release of the fuel/oxidizer combination or decreasing the energy required to decompose the polymer fuel into a gas results in more fuel mass entering the flow which in turn decreases the heat transfer back to the fuel surface. The result is that the rate of regression between different fuels does not differ much. This shows up in the mass transfer parameter, B, which is used to characterize each fuel/oxidizer combination.

Regression rate primarily depends upon the oxidizer mass flow rate per unit area, G. This is show in the regression rate equation [Ref. 3, pg. 5-9].

$$\dot{r} = \frac{0.036 \cdot G_{oxidizer}^{0.8} \cdot B^{0.23} \cdot \left(\frac{L_g}{\mu}\right)^{-0.2}}{\rho_{fuel}} \cdot \left(\frac{\bar{\rho}}{\rho_e}\right)^{0.6} \tag{2.26}$$

Where

B	mass transfer number
$G_{oxidizer}$	mass flux of oxidizer per unit area, $\dot{m}_{ox} / A_{port}$, lbm/in^2-sec
L_g	grain length in inches
$\dot{r}$	regression rate, in/sec
ρ_{fuel}	fuel density, 0.043 lb/in^3
$\bar{\rho}/\rho_e$	ratio of average to boundary layer edge densities (~ 1.19)
μ	viscosity, 1.36e –6 lbf/ft^2-sec.

The mass transfer number, B, was taken as 9.3. This value was accurate for a PMM/Oxygen system [Ref. 3, pg. 5-7], but was also a good first estimate for a PMM/IRFNA system.

SFRJ

Mady and Netzer, [Ref. 7], showed that the regression rate of a PMM SFRJ could be modeled by,

$$\dot{r} = 0.0043 \cdot G_{air}^{0.38} \cdot P_c^{0.29} \tag{2.27}$$

where,

G_{air} air mass flux, lb/sec-in^2
P_c chamber pressure, psi
$\dot{r}$ regression rate, in/sec

F. GRAIN GEOMETRY

General

Determining the grain geometry posed the most difficult problem of a H/SFRJ design. Both propulsive modes were dependent on burning surface area and port area; the SFRJ mode was also dependent upon chamber pressure as shown in Eqn. (2.27). The goal of the grain design was to make the burning surface area of the booster at burn out match the area required by the sustainer at start up and also to meet the thrust requirements of both booster and sustainer. Some of the physical parameters that could be varied were grain length, case thickness, F/O ratio, perimeter, and configuration of the grain. Unfortunately, these factors were all coupled and could not be adjusted independently. Therefore an iterative approach to grain design was called for.

The easiest configuration would have been if the grain were cylindrical. However, the required grain length for the hybrid boost phase was far longer than that required by the SFRJ sustainer. Since the desired end result of the grain design was to produce a given mass flow rate given by

$$\dot{m}_{fuel} = \dot{r} \cdot A_b \cdot \rho_{fuel} \tag{2.28}$$

and hybrid rockets have very low regression rates (close to 2.5 mm / second in this study), the burning surface area had to be increased to compensate.

This could be done by increasing the overall grain length or by using multiple ports as shown in Fig. 2.4.

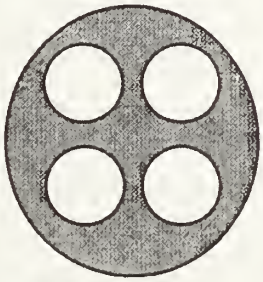

Figure 2.4 Multiport Grain

Multiple-port grains are typically used in large hybrid rockets. Small diameter tactical motors may not be able to take advantage of multiporting. If the minimum allowable port diameter is 1 in. then only three ports would fit within the missile. Multiporting also ensures that some burnout fuel sliver will occur. In a tactical missile this fuel waste decreases the chamber port area. This, in turn, increases the chamber Mach number in the sustainer which is also undesirable.

Choosing a spoked grain for both the SFRJ and hybrid modes allows the overall grain length to be less than if a cylindrical grain were chosen. A spoked grain also has much less fuel sliver than a multiple-port grain. However, because of the small regression rate and the low burn time when used as a tactical missile booster, the hybrid web must be extremely thin: approximately 3.5 mm. Using a wagonwheel configuration for the hybrid that burns out into a cylinder for SFRJ operation results in a grain with a few long slender spokes or many short spokes that are very closely spaced.

Because a hybrid rocket depends on burning within the boundary layer, using small spokes was deemed unworkable: it was felt that flow would not reach into the closely spaced spokes to promote good combustion. Long, slender pieces were liable to break off during operation.

Shortening the grain length such that a spoked grain was necessary for both modes of operation resulted in a workable solution. This is shown in Fig. 2.5.

Figure 2.5 Final Configuration

In the concept illustrated above, the spokes were large enough to prevent breakup and widely spaced enough to promote fuel pyrolysis. For performance calculations, it was assumed that the regression rate would be uniform at all points of the grain, even though it was more likely that the top of the spokes would regress more quickly because of their exposure to the relatively oxidizer rich core flow. The actual iterative procedure used for finding an acceptable grain is described below.

Sizing

Average quantities for regression rate, port area, burning area, etc. were used to calculate the required grain configuration. As a starting point, a value for the length of the fuel grain was chosen. This sets the chamber port area for a given mass of PMM fuel (determined from Eqn. (2.4) and Eqn. (2.10). For this investigation, the grain length output from the ramjet design program was used. Next, an average value of mass flux, $\bar{G}$, had to be obtained, where

$$\bar{G} = \frac{\bar{\dot{m}}_{oxidizer}}{\bar{A}_p} \tag{2.29}$$

Having $\bar{G}$ allowed the regression rate to be calculated. Knowing the regression rate and required average fuel flow yielded the average required burning surface area ($\bar{A}_b$) from Eqn. (2.28). The required perimeter (P) was then found from

$$P = \frac{\bar{A}_b}{L_g} \tag{2.30}$$

It is this perimeter that is used to determine how many constant-width spokes are required by the grain. The number of spokes, n, given by

$$n = \left\lceil \frac{P - \pi \cdot (D - 2 \cdot web_{boost})}{2 \cdot h} \right\rceil \tag{2.31}$$

was rounded up. In this equation, the web was simply,

$$web_{boost} = \bar{\dot{r}}_{boost} \cdot t_{boost} \tag{2.32}$$

and D was the internal diameter of the booster at burn out. The height, h, and width, w, of the spokes were initially selected as twice the thickness of the web, but could be adjusted somewhat.

The procedure for designing the SFRJ grain was very similar to that described above. In this case, D, was the outer missile diameter minus the wall thickness required for structural integrity. The initial and final port areas were calculated and Eqn. (2.29) was used to obtain an average mass flux. Then the regression rate for the SFRJ was calculated using Eqn. (2.27). Finally, the burning surface area required by the SFRJ was compared to the actual surface area provided by the designed grain. The actual burning surface area (A_b) was given by,

$$A_b = L_g \cdot \left[\pi \cdot (D - 2 \cdot web) + 2 \cdot n \cdot h\right] \tag{2.33}$$

Reconciliation of the burning area at booster burnout and sustainer initiation was made by iterating on grain length and the height of the spokes. The procedure was set up very effectively in a spreadsheet which could automatically iterate toward a solution.

G. CHECK OF GRAIN GEOMETRY

A check of the grain geometry was made by "burning" it in a simulation of boost and sustain modes. A small increment of web burned was translated into a variation in port area, burning surface area, etc. Port geometry and oxidizer flow rate yield the fuel flow for the booster through Eqn. (2.26) and Eqn. (2.28). Fuel-oxidizer ratio was then computed and was input into PEPCode94. Outputs from the code were T_{t4} (total temperature at the grain exit), γ, R, Isp.

Thrust during this 'web step' was calculated using

$$\text{thrust} = \text{Isp}_{\text{jet}} \cdot \eta_{\text{Isp}} \cdot \dot{m}_{\text{total}} \cdot g_o \tag{2.34}$$

Also, the time interval was calculated using

$$\text{time} = \frac{\text{web}}{\dot{r}} \tag{2.35}$$

Total impulse was then given by

$$I_t = \sum \text{Thrust} \cdot \text{time} \tag{2.36}$$

I_t was then compared to the required value for the boost phase. A similar process was followed for the sustainer.

If a nozzle made of PMM were used instead of a fixed area nozzle, it would be expected that the throat diameter would increase over the course of the hybrid operation. As a first approximation it was decided to model the regression rate of the throat much like the fuel grain,

$$\dot{r} = \frac{0.036 \cdot G_{\text{throat}}^{0.8} \cdot B^{0.23} \cdot \left(\frac{L}{\mu}\right)^{-0.2}}{\rho_{\text{fuel}}} \cdot \left(\frac{\bar{\rho}}{\rho_e}\right)^{0.6} \tag{2.37}$$

where G_{throat} was given by

$$G_{\text{throat}} = \frac{\dot{m}_{\text{oxidizer}}}{A_{\text{throat}}} \tag{2.38}$$

The question arose as to what length scale would be used in Eqn. (2.37). It was decided that the grain length would be used as a first approximation. This assumption would then be checked by experiment.

For proper operation of the sustainer, it was required that the varying area throat open up to the design point and no more. During the boost phase, if it is found that the throat opens more than is required for sustainer operation then an insert must be installed that will check the regression of the throat. This insert may be made of carbon phenolic or some other material that is resistant to erosion. Fig. 2.6 illustrates the concept.

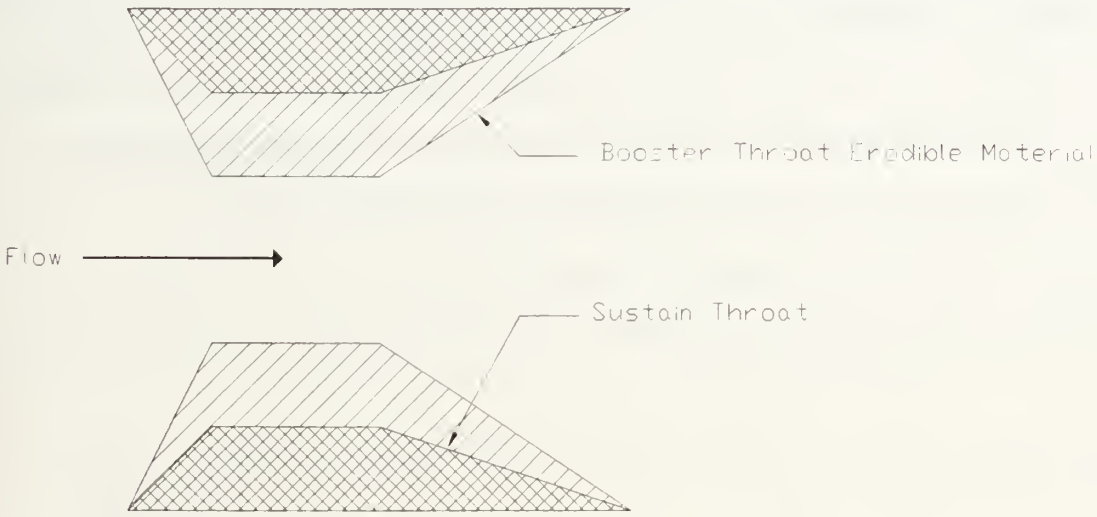

Figure 2.6 PMM Nozzle Concept

H. CHAMBER MACH NUMBER

To ensure proper flame stabilization in the SFRJ, the chamber Mach number should not be much greater than 0.3. To determine the Mach number in the chamber the following expression was used;

$$\dot{m}_{total} = P_c \cdot A_p \cdot M_c \cdot \sqrt{\frac{\gamma}{R \cdot T_c}} \tag{2.39}$$

where T_c was taken to be approximately given by the average total chamber temperature,

$$T_t = \frac{T_{t2} + T_{t4}}{2} \tag{2.40}$$

and T_{t2} was the inlet diffuser stagnation temperature.

R, γ, and T_{t4} were average quantities found using PEPCode94. According to Eqn. (2.39), the highest chamber Mach number would occur at the beginning of the sustain phase when the port area of the chamber is smallest. If the Mach number in the chamber turned out to be too high it could be reduced in several ways; but only with negative tradeoffs. First, the fuel-air ratio of the sustainer could be increased towards stoichmetric. However, more fuel must be carried if this were done. Second, the chamber port area could be increased if the grain length is increased to maintain the same fuel volume. Unfortunately this action effects the operation of the booster. Booster regression rate, and hence, mass flow rate, dropped as chamber port area was increased. The increased grain length counters this affect somewhat by increasing the burning surface area, and mass flow, but overall booster performance decreases.

III. ANALYTICAL RESULTS: INITIAL DESIGN

A. GENERAL

In this chapter the performance of PMM as a fuel is discussed for both hybrid rocket and SFRJ modes. The weight of the PMM-fueled H/SFRJ required to perform the mission is then compared to that of the conceptual IRR produced by Ramjet 2. The configuration of the grain is presented, along with the thrust and total impulse predicted by simulation.

B. PMM PERFORMANCE

As a hybrid rocket fuel, PMM has excellent performance when used with oxygen, as is clearly illustrated in Fig. 3.1 and Fig. 3.2. Performance with IRFNA is considerably lower.

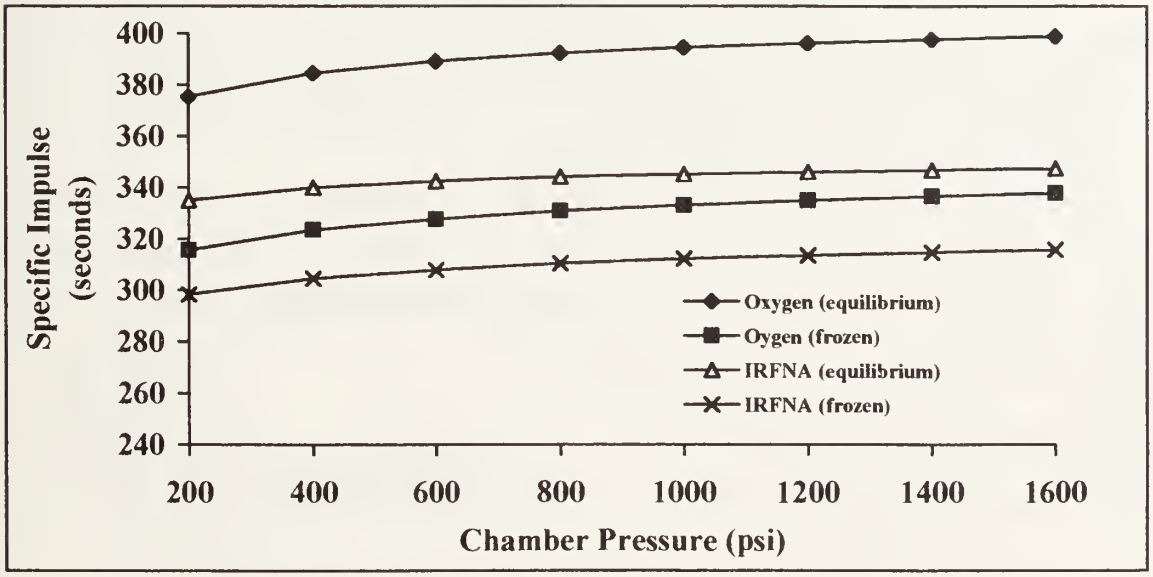

Figure 3.1 Specific Impulse vs. Chamber Pressure ($\Phi = 1$)

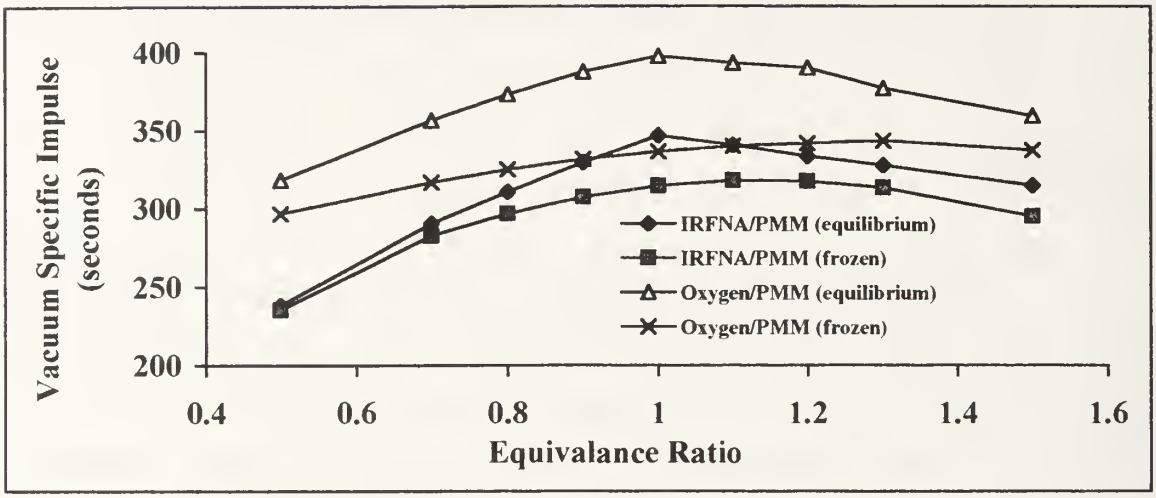

Figure 3.2 Specific Impulse vs. Equivalence Ratio

The small variation of specific impulse with chamber pressure, as shown in Fig. 3.1 is important to consider. It means that low chamber pressures, relative to a solid rocket, are usable without unduly compromising performance. Reducing chamber pressure also positively affected the weight of all pressurized tanks by decreasing the required wall thickness. For this design a chamber pressure of 1100 psi was chosen.

Although Fig. 3.1 and Fig. 3.2 show that PMM has excellent performance with oxygen, it is usually more important to consider density specific impulse in tactical missiles due to their small size and diameter. Fig. 3.3 shows that IRFNA is clearly superior in this regard (oxygen pressure = 2200 psi).

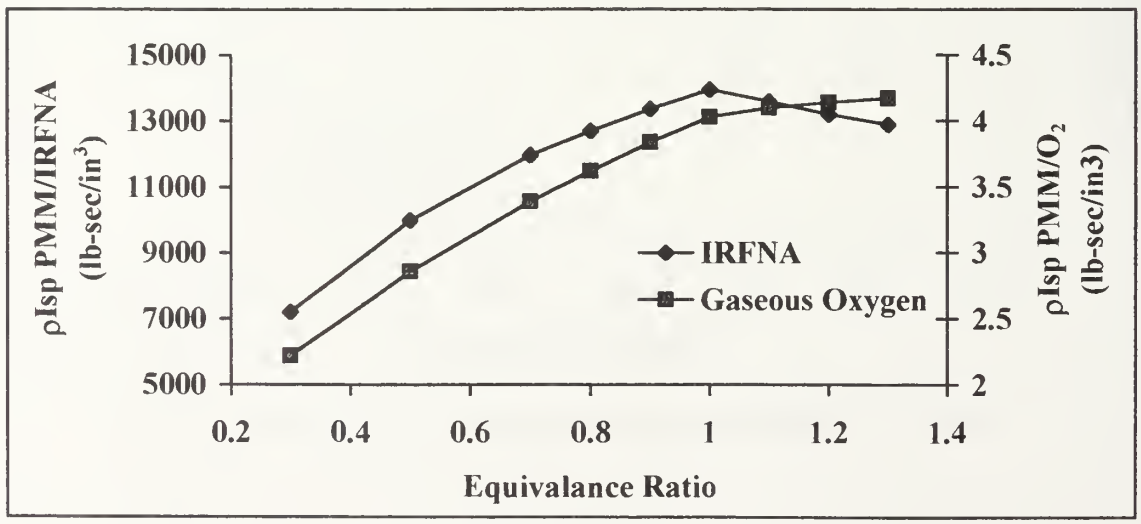

Figure 3.3 Density Specific Impulse vs. Equivalence Ratio

The much lower density specific impulse for the oxygen / PMM system implied that a large volume would be required for tankage.

As a fuel for the SFRJ, PMM has relatively low performance (Fig. 3.4).

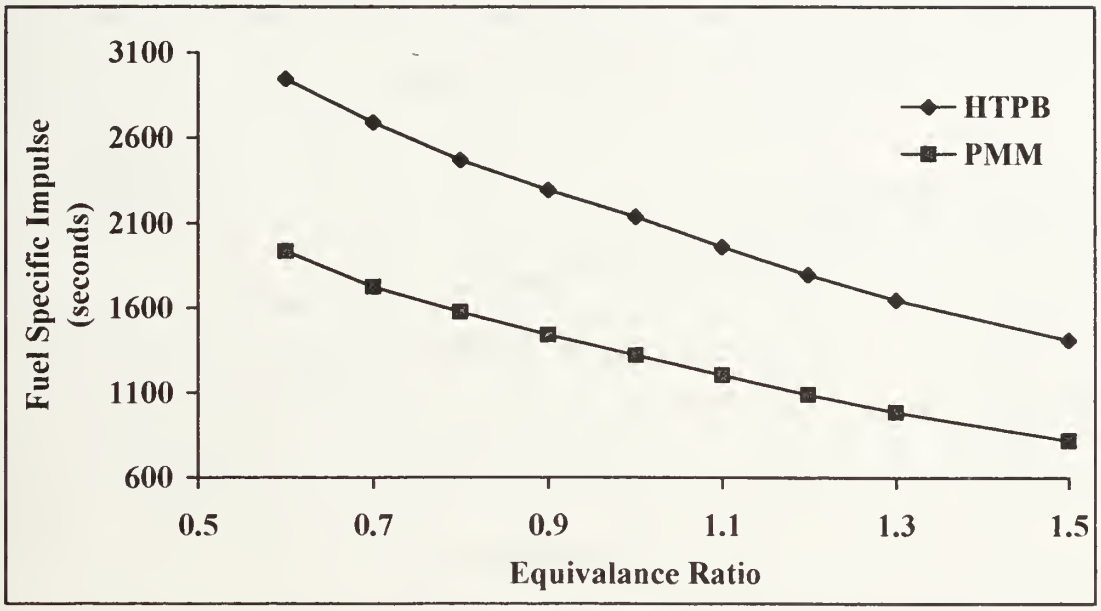

Figure 3.4 Sea Level Fuel Specific Impulse PMM/Air vs. HTPB/Air

Since UTX 18188 (used in Ramjet 2) was not available as a fuel in PEPCode94 for analysis, a similar hydrocarbon fuel, HTPB, was calculated and the results are compared in Fig. 3.4. PMM has a lower fuel specific impulse because it contains a rather high percentage of oxygen. Its chemical composition is $C_5H_8O_2$. In contrast, HTPB has the composition, $C_{73}H_{103}O$. The implication is that a larger amount of PMM will be required to accomplish the mission than if UTX 18188 or HTPB is used as a sustainer fuel.

C. WEIGHT

Booster

An optimization was conducted to minimize the amount of booster fuel. Reducing the booster fuel to the minimum value was vital to obtaining a grain design. If too much PMM was in the booster, then a grain which had the appropriate surface area at booster burnout was not possible. The thin web required by the low hybrid rocket

regression meant that a large burning surface area was required and this burning surface area at burn out would be larger than that required for the sustain phase. Choosing a lean F/O setting was the simplest way to reduce booster weight. Fig. 3.5 illustrates how booster propellant weight varied with design altitude for the conceptual 5" IRR and for a H/SFRJ calculated using the methods in the previous chapter.

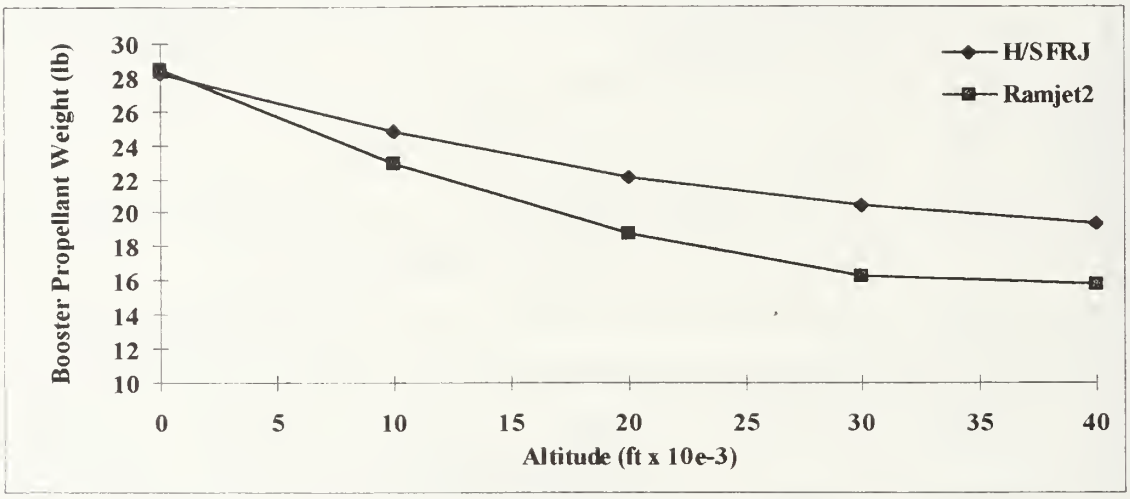

Figure 3.5 Booster Weight Comparison of H/SFRJ and IRR

At first glance the PMM/IRFNA system has a 7 - 10 lb. disadvantage vis-à-vis the IRR. This disadvantage is compounded when the tankage required by the oxidizer is taken into account.

Tankage

A substantial portion of the weight of the H/SFRJ was tied up in the required tankage. The required mass was particularly high when gaseous oxygen was used. Fig. 3.6 shows the tank weights for a 1300 psi regulated-pressure IRFNA and a 5000 psi blowdown oxygen system. A 200 psi differential between tank and combustion chamber was maintained when using IRFNA to minimize any chamber-injector coupling.

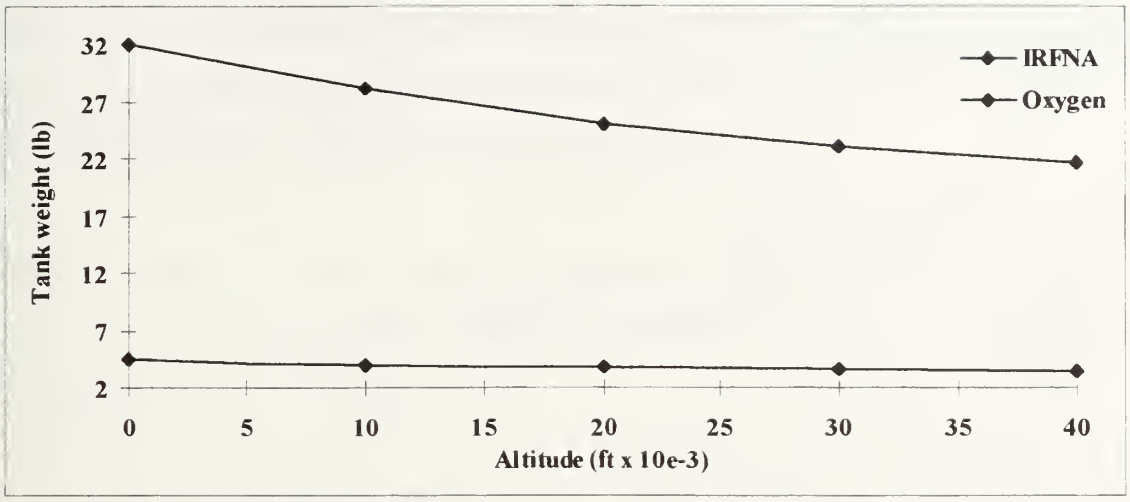

Figure 3.6 Tankage Weight for H/SFRJ

Another important concern was the extra length that a H/SFRJ must have to accommodate tankage. Tank length for a gaseous oxygen system is prohibitive as shown in Fig. 3.7.

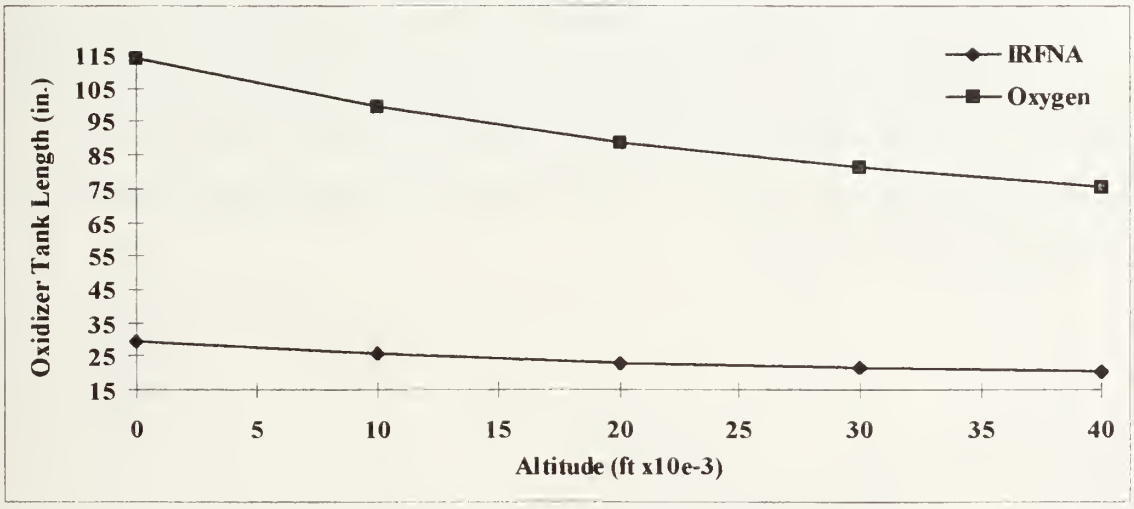

Figure 3.7 Oxidizer Tank Length

The large tank length occurred because of the 5" diameter constraint. Because of the large tank length and weight associated with gaseous oxygen, it was eliminated from further consideration.

Sustainer

As expected, the mass of the sustainer fuel was substantially more than that required for the IRR (Fig. 3.8). The required SFRJ fuel weight was higher than the

program value since the latter used an HTPB-like fuel instead of PMM.

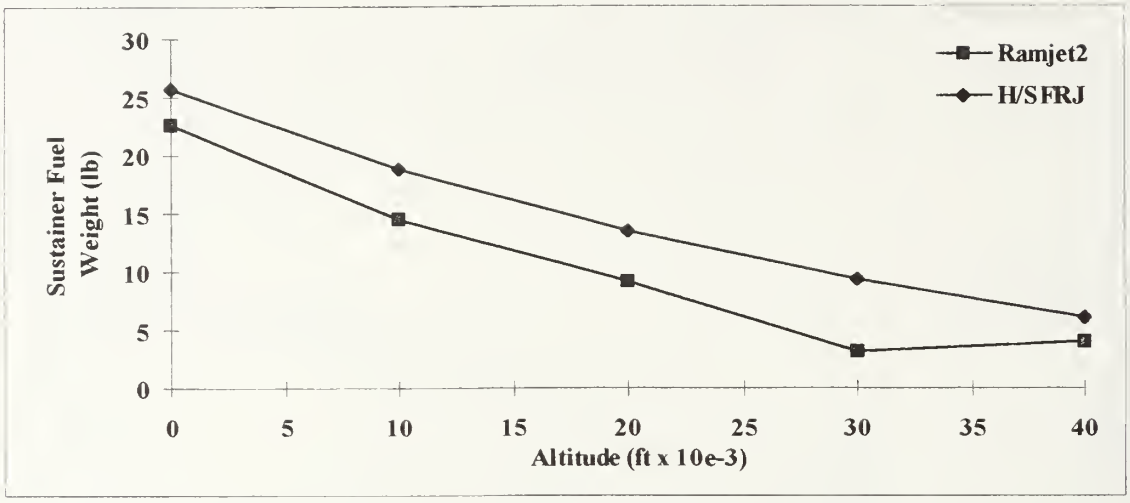

Figure 3.8 Sustainer Fuel Weight H/SFRJ vs. IRR

Case

The replacement of the metal case with PMM provides a significant savings in weight. It is this savings that allows the H/SFRJ to be competitive weight-wise with a conventional IRR. Case weight for the IRR is an output from Ramjet 2 and includes the weight of an insulating liner, see Fig. 1.1. The variation of the required case weight with design altitude is shown in Fig. 3.9.

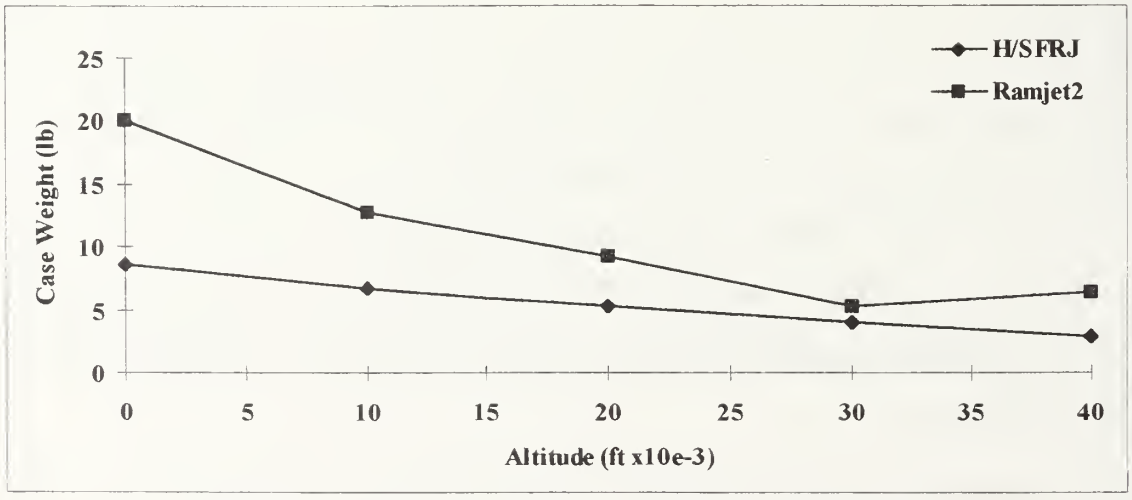

Figure 3.9 H/SFRJ and IRR Case Weight Comparison

The saving is particularly significant at lower altitudes because a greater reduction in grain length (and its metal casing) is possible. This is another interesting

phenomenon caused by "layering" the hybrid booster fuel over the sustain fuel as shown in Fig. 2.5. By layering the fuel the required grain length is shortened, and the booster perimeter goes up to compensate to keep the burning area the same.

$$A_b = L_g \cdot P \tag{3.1}$$

However, because port area also decreases, regression rate of the hybrid booster increases. This allows the burning surface area required by the booster to match the startup condition of the sustainer. Therefore, shortening the grain is beneficial in both obtaining the required booster regression rate and in shortening the overall grain length.

At high altitudes the required amount of sustainer material was much less than that of the booster and the required burning surface area of the booster was much greater than that required by the sustainer. Thus, it becomes much more difficult to match the burning area at booster burnout with that required by the sustainer.

A comparison of the total H/SFRJ and IRR propulsion system weights, as depicted in Fig. 3.10, indicates that the H/SFRJ cannot quite match the IRR in performance and weight in the tactical missile application using PMM as a fuel.

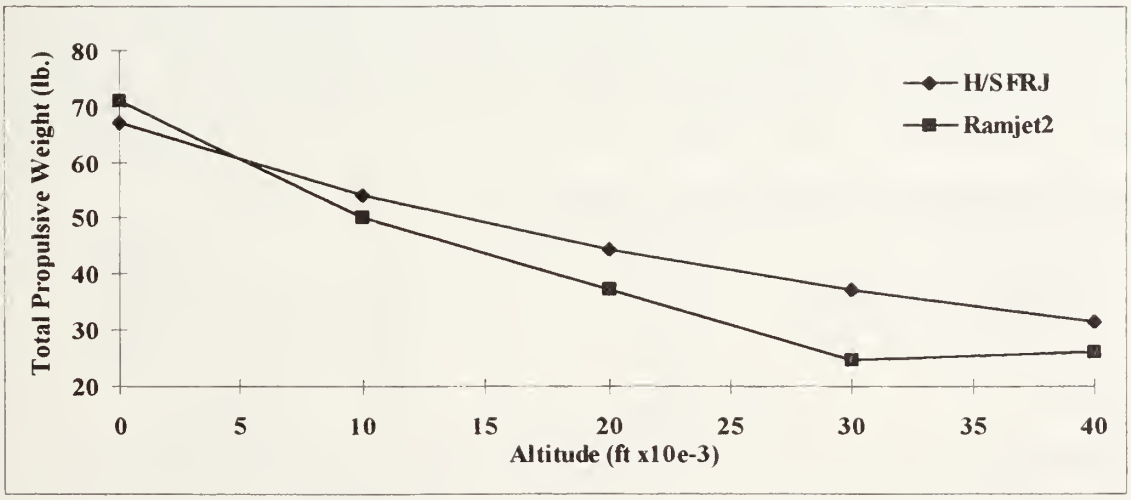

Figure 3.10 Total Propulsive Weight Comparison IRR vs. H/SFRJ

D. INITIAL H/SFRJ GRAIN DESIGN

An initial H/SFRJ propulsion system based upon the methods of the previous chapter was designed. For the 20,000 ft, Mach 2, 20 nm. mission the H/SFRJ had the characteristics shown in Table 3.1.

Grain Length (in.)	51.9	Number of Spokes	3
Mixer Length (in.)	10.0	Spoke Height (in.)	0.904
Equivalence Ratio	0.75	Spoke Width (in.)	0.861
Equivalence Ratio	1.0	Initial Burn Area ($in.^2$)	914.5
PMM Total (lb.)	17.7	Initial Port Area ($in.^2$)	9.48

Table 3.1 H/SFRJ Missile Characteristics

E. PERFORMANCE OF A H/SFRJ GRAIN

In a simulated test, the H/SFRJ demonstrated performance comparable to a IRR. During boost, the hybrid-rocket thrust decayed slightly over time as the port area increased which reduced G. This was expected. Also, F/O decreased for the same reason. Burning surface area increased slightly, but not near enough to compensate for the effect of reduced G. The thrust-time profile for the hybrid rocket using a fixed area nozzle is shown below. Ramjet 2 assumes a constant thrust-time profile for the solid propellant rocket booster, and this is also plotted in Fig. 3.11 for comparison.

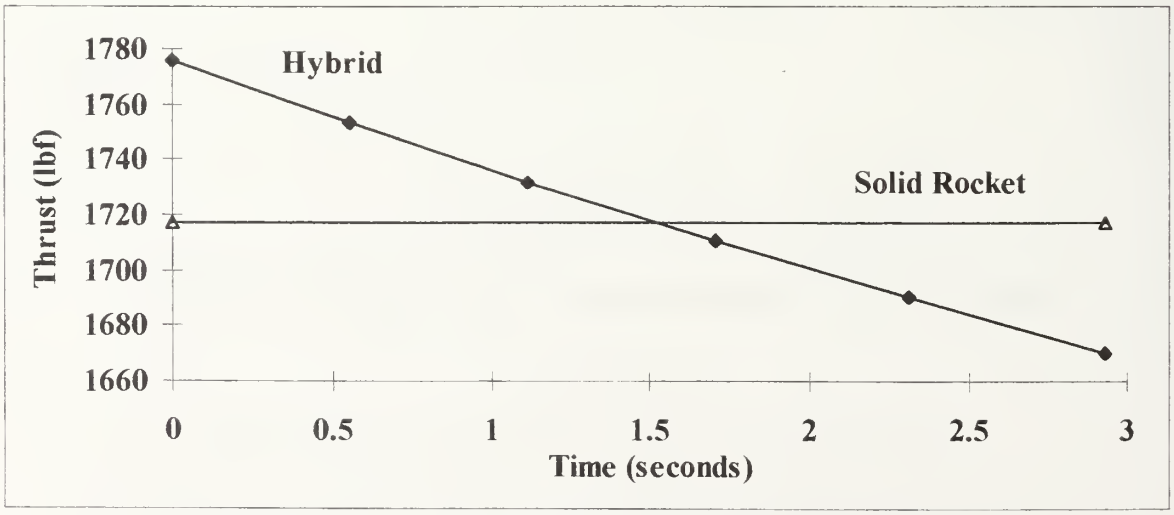

Figure 3. 11 Thrust-Time Profile: Fixed Area Nozzle

The thrust profile for the hybrid compares quite well with IRR using a fixed nozzle. If the throat area of the nozzle was allowed to increase according to the model given in the previous chapter, then a slightly different profile occurs, which is shown in Fig. 3.12.

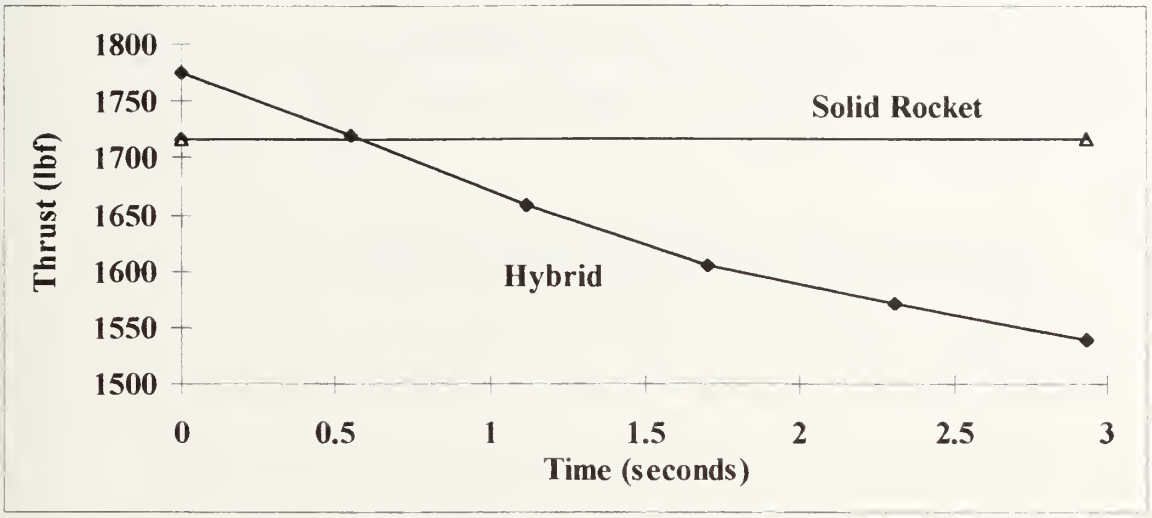

Figure 3.12 Booster Thrust-Time Profile: Variable Area Nozzle

The total impulse at the end of boost was still within 5% of the value required by the Ramjet 2 code for this missile. The total impulse required by the design code was compared to the hybrid design for a fixed and an eroding nozzle, and the results are shown in Table 3.2.

	Total Impulse (lbf - sec)	Percent Difference
Ramjet 2	5031	0
Hybrid: Fixed Area Nozzle	5111	+1.6
Hybrid: Eroding Nozzle	4869	-3.2

Table 3.2 Booster Total Impulse

The nozzle throat area increased substantially using the assumed regression rate model, but the final throat diameter predicted was still much smaller than the design throat size required by the sustainer. It had been hoped that the nozzle throat would quickly open up when the sustainer fired. However, simulation using the sustainer regression rate equation indicated that the throat would regress very little. Testing is required to determine the actual throat erosion rate because the regression rate models have not been validated at near-sonic flow conditions.

IV. EXPERIMENTAL APPARATUS AND PROCEDURES

A. GENERAL

The overall goal of the experiments was to gain confidence in certain assumptions made in the analytical portion of this investigation. Specifically, the desired information for the hybrid booster was:

1. The regression-rate behavior of a spoked grain.
2. Assurance that combustion efficiency in a PMM motor would not be unreasonably low (it would be expected to be slightly low in the subscale motors used in this investigation).
3. The validity of the regression-rate model used for a erodible PMM nozzle throat.
4. The ability to transition from the hybrid-boost mode to SFRJ-sustain mode without a second ignition source.

To carry out these experiments, small-scale PMM motors were constructed and run in the Naval Postgraduate School Combustion Laboratory. The apparatus and procedures used during testing are described in the sections that follow.

B. APPARATUS

The hybrid-rocket and SFRJ test facility is comprised of a 3000 psi air supply, a hydrogen/oxygen vitiated air heater, a thrust stand, oxygen supply, nitrogen supply, and torch ignition systems for the air heater and the combustor. Gaseous oxygen was used for hybrid runs. Due to handling constraints at the lab, inhibited red fuming nitric acid, IRFNA, could not be used. Fig. 4.1 provides a schematic of the overall test apparatus.

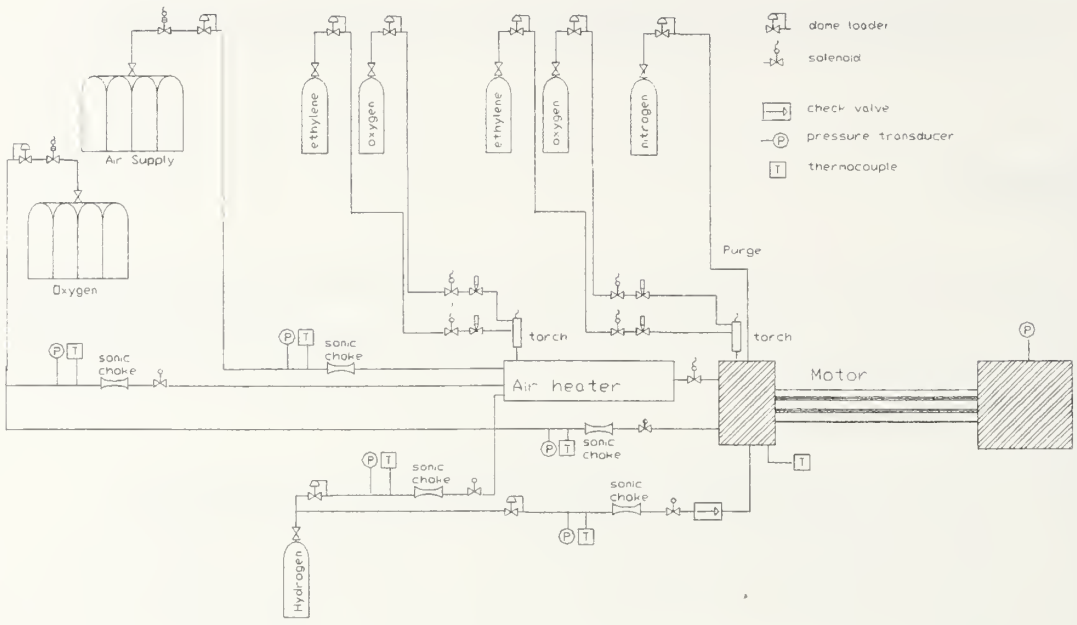

Figure 4.1 Schematic of Test Apparatus

Test Stand and Hybrid / SFRJ Motor

The hybrid / SFRJ motor consisted of three main sections: the head-end assembly, the fuel grain and the aft-end assembly (including the aft mixer). Fig. 4.2 provides a sketch of the motor.

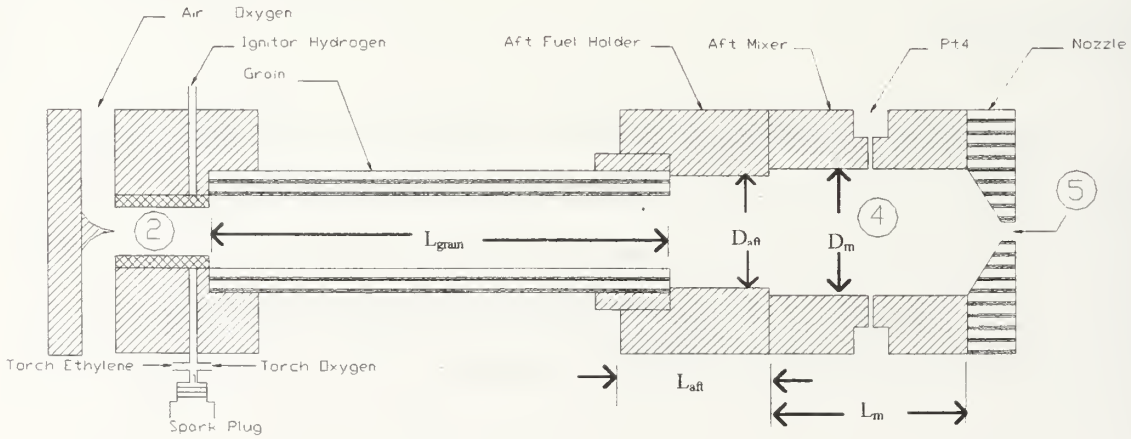

Figure 4.2 Hybrid / Solid-Fuel Ramjet Motor

The head-end assembly functioned as the fuel grain holder and was ported to allow introduction of oxygen, heated air, and nitrogen. The head-end contained a thermocouple probe for measuring T_{t2} and a pressure tap for P_{t2}. Oxygen pressure was

available up to 2000 psi from three high-pressure tanks acting though a manifold. Nitrogen was used to quench the flame following test runs. The aft-end of the fuel holder was a 2.1 in. inner diameter (D_{aft}) with a length of 2 in. (L_{aft}). The mixer section had a diameter of $D_m = 2.6$ in. The total length of the mixer (L_m) was 4 in. The entire motor assembly was mounted on a thrust stand as shown in Fig. 4.3. All connections to the motor were made using stainless steel flex lines to avoid interfering with thrust measurements. Thrust was measured by a strain-gauge load cell. All gaseous flow rates were regulated using sonic chokes.

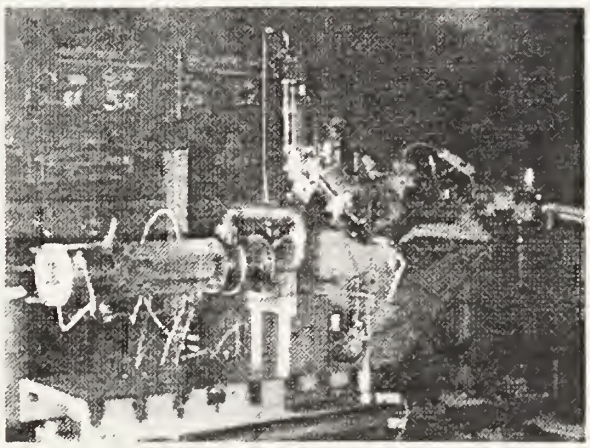

Figure 4.3 Test Stand

Ignition System

The motor ignition system utilized an ethylene and oxygen torch that ignited the air or oxygen-hydrogen mixture at the head-end of the fuel grain. Both ethylene and oxygen were supplied from high pressure tanks. The ethylene / oxygen torch was ignited electronically with a standard automotive spark plug. A separate ignition system, using ethylene / oxygen, was used for the SFRJ air heater.

Air Heater

A vitiated air heater was used when in the SFRJ mode to increase the stagnation temperature, T_{t2}, of air flowing into the fuel grain. Temperatures up to 1100 R could be generated, simulating conditions up to approximately Mach 2.7 @ 20,000 ft. altitude. Makeup oxygen was introduced to maintain the correct oxygen mole fraction.

Fuel Grain

All fuel grains were 100% polymethylmethacrylate (PMM). Inner diameters of the grains varied from 1.5" to 1.8" diameter. PMM sections came in 8" and 12" lengths which were cut and joined with diethylene chloride to obtain desired grain lengths. Fuel-density measurements were made to confirm uniformity of the test material.

To maximize the use of resources, used grains were bored out to a new inner diameter, pressure tested with cold air, and reused as necessary.

Data Acquisition System

Data acquisition was via a HC1801 data collection card in a PC. Keithly-Metrabyte's Viewdac™, was used to manage the rate (100 Hz) and duration of data acquisition.

Video

A Panasonic FL-300 video camera was used to record each run in order to spot potential abnormalities. An annotation system provided timing to be recorded during the run. The camera was utilized with a shutter speed of 1/1000 second and a frame rate of 30 per second.

C. TEST PROCEDURES

Pre-run Activities

Prior to each run, the weight of the fuel grain was measured (to be used later with a post-fire measurement to determine average regression rate). Fuel grain length, inner diameter, and the dimensions of any spokes running the length of the grain were measured. The nozzle throat diameter was also measured.

Using the above information, the grain port area could be readily determined. Grain port area and the mass flow of oxygen (and air for combined hybrid / SFRJ firings) yielded the mass flux per unit area, G, and allowed the regression rate to be predicted using Eqn. (2.26) or Eqn. (2.27). Oxygen mass flow, nozzle throat size, and grain length

were chosen to maintain chamber pressures between 300 and 500. 300 psi was chosen as the lower limit to avoid low pressure effects on the fuel regression. 500 psi represented a safe upper limit on chamber pressure for this facility.

The thrust stand was calibrated immediately prior to firing due to the stand's extreme sensitivity to disturbance. A regression fit of the calibration data was obtained using Microsoft's EXCEL spreadsheet.

The final pre-run activity was to set the amount of time that various gases (oxygen, air, purge nitrogen, ignitor gases) flowed during the run. This was easily accomplished using Viewdac™. Ignition gases were timed to flow for 400 ms to ensure consistent ignition. Purge nitrogen was programmed for a 4 second run, 500 ms after oxidizer cut off.

Post-Fire

Post run activities were performed in order to determine the average fuel regression rate and combustion efficiency. Regression rate of the fuel grain was determined by two methods. The following expression was used to evaluate the regression rate based on weight loss;

$$\bar{\dot{r}} = \frac{\sqrt{\frac{4 \cdot \Delta m}{\pi \cdot \rho \cdot L} + D_i^2} - D_i}{2 \cdot \Delta t} \tag{4.1}$$

Direct measurements yielded a second measure of regression rate using,

$$\bar{\dot{r}} = \frac{\bar{D}_f - \bar{D}_i}{2 \cdot \Delta t} \tag{4.2}$$

Diameter measurements were also made on PMM nozzle throats. These measurements allowed the average regression rate to be calculated.

Combustion efficiency was based on temperature rise using the methods contained in AGARD Advisory Report 323, [Ref. 8]. To obtain combustion efficiency, the chamber total pressure, P_{t4}, was first calculated. This was done in two different ways, using either measured P_4 or the measured thrust. Using the static pressure measurement, P_4,

$$p_{t4} = p_{4,exp} \cdot \left(1 + \frac{[\gamma + 1]}{2} \cdot M_4^2\right)^{\frac{\gamma}{\gamma - 1}} \tag{4.3}$$

M_4 and γ were determined automatically using options within PEPCode 94 with measured P_4, $\dot{m}_{fuel} / \dot{m}_{ox}$, and A_4/A_5 (internal grain to nozzle area ratio) as inputs. Using thrust measurements P_{t4}, was found using

$$p_{t4} = \frac{F_5 + p_{amb} \cdot A_5}{(1 + \gamma \cdot C_D) \cdot A_5} \cdot \left(\frac{\gamma + 1}{2}\right)^{\frac{\gamma}{\gamma + 1}} \tag{4.4}$$

where F_5 is the measured thrust using a converging-only nozzle. C_D was determined by ratioing measured flow rate to the corresponding one-dimensional, isentropic flow rate from pre-firing flows of air with a choked exhaust nozzle. Having determined total pressure at station 4, c^*_{exp} was evaluated using

$$c^*_{exp} = \frac{p_{t4} \cdot A_5 \cdot C_D}{\dot{m}_4} \tag{4.5}$$

which allowed the total temperature at station 4 to be calculated from

$$T_{t4,exp} = \gamma \cdot \left(\frac{2}{\gamma + 1}\right)^{\frac{\gamma + 1}{\gamma - 1}} \cdot \frac{c^{*\,2}_{exp}}{R_4} \tag{4.6}$$

R_4 was calculated using PEPCode94 in the same step as M_4 and γ. The combustion efficiency based on temperature rise was then calculated using

$$\eta_{\Delta T} = \frac{T_{t4,exp} - T_{t2}}{T_{t4,th} - T_{t2}} \tag{4.7}$$

where the theoretical value of total temperature, $T_{t4,th}$, was obtained from PEPCode94.

Transition Test

The object of this test was to determine whether a hybrid rocket with a step-inlet and a spoked-grain could transition to a SFRJ using PMM without a secondary ignition system. The other objective was to simulate a nozzle that erodes during hybrid operation but stops regressing at the sustainer design nozzle size. This was done using two

separate nozzles. A smaller PMM nozzle was allowed to erode. The second nozzle, constructed of stainless steel, was mounted directly behind the PMM nozzle as shown in Fig. 4.4.

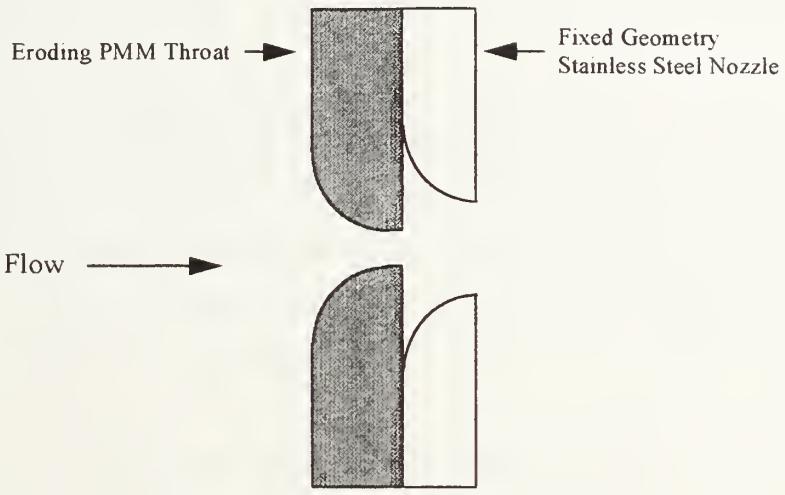

Figure 4.4 Transition Test Nozzle Arrangement

A spoked grain was used. This allowed the interaction between the inlet and spokes to be examined. A stainless steel insert was used at the head-end of the fuel grain to provide an inlet diameter-to-grain inner-diameter ratio of 0.33. This ratio was chosen to provide good flameholding characteristics for the PMM SFRJ sustainer.

After pre-firing activities, the SFRJ vitiator was actuated and allowed to come up to its final operating temperature of 420 K. This air was dumped overboard during warm-up and during the hybrid rocket firing.. The test sequence was then initiated with the hybrid booster set to burn for 1 second. The hybrid oxygen flow valve was closed at the same time the air flow valve was opened. Combustion time for the SFRJ was set at 5 seconds.

V. EXPERIMENTAL RESULTS

A. GENERAL

Tests were successfully conducted that confirmed the validity of Eqn. (2.26) for the hybrid regression rate of PMM. Combustion efficiency turned out to be low, but this was expected in the small motor that was used. Nozzle-throat regression tests confirmed that adequately high regression rates do occur during hybrid operation. Successful hybrid rocket-SFRJ transition was also demonstrated..

B. REGRESSION RATES / COMBUSTION EFFICIENCY

It was found that the regression rate of the fuel grain during hybrid-rocket operation was slightly higher than predicted by the model developed by UTC [Ref. 3]. These values are listed in the table below. In two cases the difference between the predicted and actual values was significant. The first of these two cases, run #2, was conducted with a very low oxidizer mass flux, G. This low value of G resulted in a very low regression rate that was characterized by subsurface melting of the grain. Video analysis showed this material sloughing off the wall of the fuel grain. This was believed to be the cause of the disparity.

Run	Grain Length (in)	G (lb/in^2-sec)	F/O	$\dot{r}_{actual}$ (in/sec *10e3)	$\dot{r}_{predicted}$ (in/sec *10e3)	Percent Difference
1	16	0.0296	0.265	4.14	4.31	- 4%
2	16	0.0210	0.451	5.60	3.44	63%
3	16	0.0760	0.185	9.28	9.20	0.9%
4	36	0.0713	0.549	9.49	7.40	28%
5	24	0.0856	0.386	10.53	9.29	13%
6	24	0.0737	0.393	9.65	8.30	16%
7	11.75	0.0105	0.308	14.48	12.64	14%
8	18.25	0.0724	0.229	9.14	8.58	7%

Table 5.1 PMM-O_2 Hybrid Rocket Fuel Regression Rate Data

The second case, Run #4, had a very long tail-off period following oxygen shutdown. The tail-off was observed to be 1.6 seconds in duration based upon the video taken during the run. The cause of this is unknown.

The seventh run conducted was significant in that a spoked grain was tested. The spoked grain showed little difference in average regression rate from that of the other tests. The spokes showed negligible tapering from top to bottom after the run. This was somewhat unexpected. It had been thought that the relatively oxygen-rich core flow would yield a slightly higher change in width at the top of the spoke compared to that of the bottom. The even regression of the spokes validated the procedures used to compute the fuel flow rate in the design calculations.

The calculated combustion efficiency based on temperature rise in the combustor varied considerably. The data for those runs using eroding nozzles is given in Table 5.2.

Run #	Efficiency (total pressure from measured pressure and PEPCode)	Efficiency (total pressure computed from measured thrust)
4	73.7	81.47
5	82.3	90.7
6	77.5	82.7
7	84.8	88.3
8	75.4	77.8

Table 5.2 Combustion Efficiency With Varying Area Nozzle Throat

Because the area of the nozzle varied during the firing, an average nozzle area was used in Eqn. (4.4) and Eqn. (4.5). This was a source of error whose magnitude was undetermined. Also, the shape of the nozzle changed over the course of firing from converging to converging-diverging. This would increase thrust and introduce an error into Eqn. (4.4), which was derived for a converging nozzle only.

C. NOZZLE REGRESSION

In the hybrid rocket tests, the mass flow of oxidizer was varied as was the equivalence ratio. In tests #4 through #8, each PMM nozzle throat ended in a 0.5" flat

section. Due to the long "sonic" sections, the throats of these nozzles regressed nearly the same amount regardless of operating conditions. If regression rate in the region of the throat was fundamentally the same as regression in the fuel grain, then the expected final throat diameter would be much higher. Test #9, using a more realistic 0.1 in. flat throat section, opened up much more, indicating that the internal configuration of the nozzle plays a role in how much the throat regresses. Thus, tailoring the booster throat design should permit attainment of the desired erosion rate. Table 5.3 gives details pertinent to the tests conducted.

Run #	4	5	6	7	8	9
Equivalence Ratio	1.045	0.787	0.782	0.626	0.477	-
Oxygen Mass Flow (lb/sec)	0.128	0.155	0.144	0.139	0.183	0.169
$G_{average}$ through nozzle (lb/in^2-sec)	1.08	1.21	1.21	1.14	1.54	1.04
$G_{minimum}$ (lb/in^2-sec)	0.657	0.708	0.736	0.691	0.955	0.542
$G_{maximum}$ (lb/in^2-sec)	2.08	2.52	2.34	2.26	2.97	2.72
Initial Throat Diameter (in)	0.280	0.280	0.281	0.281	0.281	0.280
Final Throat Diameter (in)	0.498	0.528	0.499	0.506	0.497	0.693
Burn time (seconds)	2	2	2	2	2	2.5
Predicted Burn Time to Obtain Final Diameter	1.89	1.81	1.60	1.50	1.20	2.51

Table 5.3 PMM Nozzle Regression Data for Hybrid Rocket Operation

A distinct problem is determining the local value of G at a given instant of time. The equation,

$$\text{thrust} = P_c \cdot A_{throat} \cdot C_F \tag{5.1}$$

could be solved for A_{throat}, with known pressure and thrust measurements, except that the thrust coefficient, C_F, varied throughout the firing as the nozzle throat diameter and nozzle shape changed.

Because of the time-varying nature of the measured parameters, $P_{chamber}$ and thrust, and of the nozzle throat geometry and mass flow rate through the throat, it is

difficult to design an experiment that can positively identify the parameters that control the erosion of the throat.

Of the six PMM nozzles tested, all but one of the nozzles burned uniformly and maintained a circular exit. In firing the spoked grain, Run #7, very slight scalloping at the nozzle exit (but not at the throat) was produced. The irregularities in the nozzle exit were aligned with the spokes in the grain.

D. TRANSITION TEST

The transition from hybrid-rocket to solid-fuel ramjet was accomplished smoothly, demonstrating that a H/SFRJ is possible. There was no observed hesitation in ignition. It was apparent that there was enough vaporized fuel in the chamber and that the fuel grain surface was hot enough to be an ignition source for this fuel when air was added. The pressure-time trace is shown below in Fig. 5.1. The trace shows a large pressure spike that occurred due to the introduction of the sustainer air in the instant prior to the booster oxygen cutoff.

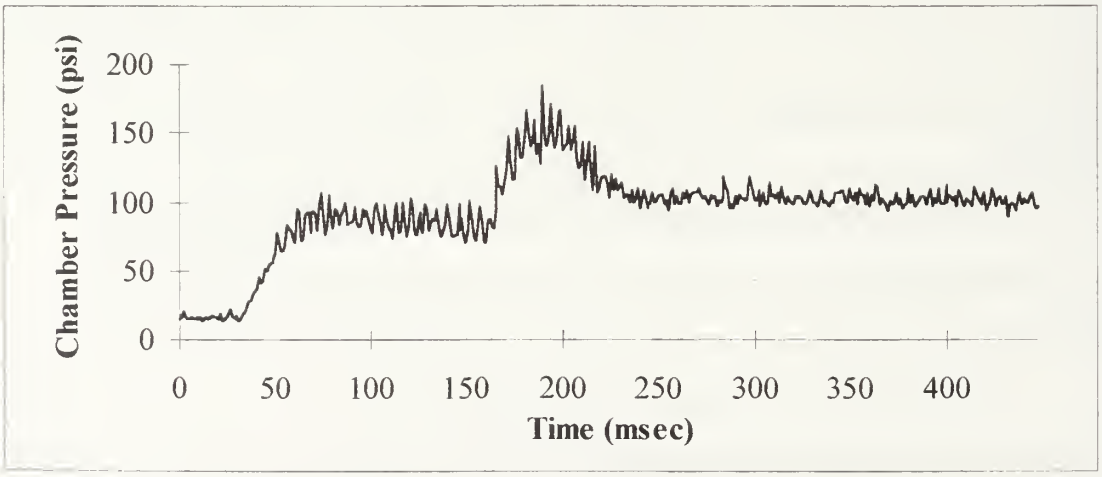

Figure 5.1 Pressure-Time Trace for Hybrid-Solid Fuel Ramjet Transition

The pressure in the hybrid rocket was low due to the large nozzle size and low oxygen flow rates that were used. The ramjet pressure was comparatively high, because the ramjet flow rate was nearly double that of the hybrid rocket.

Following the firing, the PMM nozzle was examined. The throat had regressed to an inner diameter of 0.943 in. (from an initial diameter of 0.693 in.). The relative amount of regression that occurred due to hybrid-rocket operation and that due to the SFRJ could not be determined. Further experiments will be required.

VI. CONCLUSIONS

The results of an analytical study showed that a hybrid-rocket booster can be coupled with a solid-fuel ramjet sustainer using a common fuel grain. Using a caseless design and PMM as the fuel, the missile will be longer, and slightly heavier than a missile using a conventional integral-solid-propellant booster. The primary drawbacks to using PMM are its relatively low performance as a ramjet fuel and its low regression rate during hybrid-booster operation. Metal additives could be used which boost performance, but regression rate information must be generated.

The primary advantages of a H/SFRJ design are its simplicity, especially in manufacturing, and the large amount of weight saved in eliminating the metal case. The structural capability of a caseless design was not considered in this investigation, but would be necessary to validate the concept. It may be that a caseless design is suited for missions where little maneuvering is required (bending stress) such as air-to-ground, but not for high-g maneuvering missions such as air-to-air.

The concept of using a erodible booster nozzle, although novel, appears to be workable for a hybrid-rocket booster. The hybrid-rocket booster can operate over a broad range of chamber pressure, and still deliver the total impulse necessary for a tactical missile booster. Testing certainly indicated that regression rate is largely unaffected by pressure and that an erodible throat will regress significantly.

In short, the idea of a caseless, hybrid rocket / SFRJ with an eroding nozzle is worthy of more scrutiny. Further study may very well offer up a safer, easier-to-manufacture, lightweight missile which has a much longer range than current small tactical missiles.

LIST OF REFERENCES

1. John K. Green Jr., Lethal Unmanned Air Vehicle Feasibility Study, Master's Thesis, Naval Postgraduate School, September, 1995

2. Keith J. Fruge, Design And Testing Of A Caseless Solid-Fuel Integral-Rocket Ramjet Engine For Use In Small Tactical Missiles, Master's Thesis, Naval Postgraduate School, September, 1991

3. G. A. Marxman, et. al., Investigation Of Fundamental Phenomena In Hybrid Propulsion (U), United Technology Center, November 1965

4. W. R. Anderson, et. al., Ramjet Engine And Missile Sizing Program, Ramjet 2

5. D. R. Cruise, Theoretical Computations Of Equilibrium Compositions, Thermodynamic Properties, And Performance Characteristics Of Propellant Systems, Naval Weapons Center Report NWC TP 6037, April, 1979

6. G. P. Sutton, Rocket Propulsion Elements, 6th Edition, ISBN 0-471-52938-9, 1992, Wiley & Sons, Inc.

7. C. J. Mady, et. al., Combustion Behavior Of Solid-Fuel Ramjets, Journal of Spacecraft and Rockets, Vol. 15, No. 3, May-June, 1978, pp. 131-132

8. AGARD, Experimental And Analytical Methods For The Determination Of Connected-Pipe Ramjet And Ducted Rocket Internal Performance, Propulsion and Energetics Panel Working Group 22, July 1994

INITIAL DISTRIBUTION LIST

1. Defense Technical Information Center 2
   8725 John J. Kingman Rd., STE 0944
   Ft. Belvoir, VA 22060-6218

2. Library, Code 13 2
   Naval Postgraduate School
   Monterey, CA 93943-5101

3. Dr. Kneale Marshall, Code OR/Mt 3
   Naval Postgraduate School
   Monterey, CA 93943-5101

4. Chairman, Dept. of Aeronautics and Astronautics 1
   Department of Aeronautics and Astronautics
   Naval Postgraduate School
   699 Dyer Road-Room 137
   Monterey, CA 93943-5106

5. Dr. D. W. Netzer 2
   Department of Aeronautics and Astronautics
   Code AA/Nt
   Naval Postgraduate School
   699 Dyer Road-Room 137
   Monterey, CA 93943-5106

6. Dr. Conrad F. Newberry 1
   Department of Aeronautics and Astronautics
   Code AA/Ne
   Naval Postgraduate School
   699 Dyer Road-Room 137
   Monterey, CA 93943-5106

7. Dr. R. P. Shreeve 1
   Department of Aeronautics and Astronautics
   Code AA/SF
   Naval Postgraduate School
   699 Dyer Road-Room 137
   Monterey, CA 93943-5106

8. LT Paul C. Woods 2
   P.O. Box 1150
   Ashland, OR 97520